

A PSO algorithm for biped gait planning using Spline Approximation

Zhang Qizhi Zhou Yali
School of Automation
Beijing Information & Technology University
Beijing 100192, China
{zqzbim, zhouyali6807}@yahoo.com.cn

Ge Xinsheng
School of Automation
Beijing Information & Technology University
Beijing 100192, China
gebim@vip.sina.com

Abstract—this paper discusses an optimal trajectory planning method for a compass gait biped robot. The biped robot is composed of a stance leg and a swing leg. Each step of walking locomotion is divided into two phases, i.e., the swing phase and toe collision phase. It is assumed that the toe collision is perfect plastic and occurs instantly. The motion of the swing and stance legs in swing phase is solved by the optimal trajectory planning based on the particle swarm optimization (PSO) and the spline approximation method. The performance index function is designed as the integral of weighted sum of input torque's square, each joint trajectory is approximated by a spline function. The optimal trajectory solutions are obtained by PSO method. The hip joint can be approximately passive by increasing the corresponding weighted factor, so that a smaller motor can be used at the hip joint to reduce the joint mass. Computer simulations are performed for the optimal trajectory planning method for a compass gait biped robot. Simulation results show that the proposed method is more energy-effective than the virtual gravity method.

Keywords—biped robot, optimal trajectory planning, particle swarm optimization, spline approximation

I. INTRODUCTION

In recent years, many studies have been done for realizing dynamic walking of biped robots. The available control method which is used to generate a stable walking gait is the Zero Moment Point (ZMP) method [1]. The joint trajectories are generated according to the ZMP criteria, and then the biped robot's joints are controlled to follow the trajectories by servo motors. Many biped robots have been developed by the researchers, of all these biped robots, the state-of-the-art bipedal robots should be the Humanoid robots developed in Japan [2,3], they can perform many complex motions and keep themselves stable. For present humanoid robots, the remaining key problem is the effectiveness of the humanoid robots which is limited by the amount of energy they requires. It is estimated that ASIMO's energy consumption is some 32 times greater than that of a typical human [4]. The inefficiency of energy is due to the fact that the control method of humanoid robots originates from traditional industrial robot technology, and electrical drives with high gain PD controllers are often used, which make the joints stiff [5]. Compliant actuators can be implemented in order to reduce the energy consumption of walking and running robots by exploiting the natural dynamics

of passive “spring-like” elements [5]. Passive Dynamic Walking (PDW) has been established that a suitably designed unpowered biped robot can walk down a gentle slope utilizing only gravity effect and generates a stable periodic gait [6]. The passive walker utilizes its physical dynamics and creates energy-effective walking pattern automatically. In order to walk on the level ground and to keep energy-effective, active walkers based on the passive dynamic walking are studied by many researchers [4,7-9].

The natural walking gait with minimum power consumption or minimum integral of sum of input torque's square has been calculated by the optimal trajectory planning method [9]. The natural biped locomotion with minimum integral of sum of input torque's square at all active joints is obtained by means of the optimal trajectory planning method. if input torques are minimum, the mass of actuators can be reduced, and then the walking efficiency can be raised additionally [9]. In [9], the joint motion trajectory is approximated by a set of Hermite polynomial functions and the optimal trajectory planning problem is converted into the boundary parameter optimization problem. The 7th-order Hermite polynomial approximation was used in this method, the optimal method is complex and difficult for realizing. The high-order polynomial approximation is sensitive to the coefficients estimating.

A biped gait planning method using a Particle Swarm Optimization (PSO) algorithm is proposed in this paper. The cubic spline function is introduced to approximate the joint motion trajectory. A 2D compass biped robot is selected to examine the proposed algorithm. Simulation results show that the PSO algorithm for biped gait planning using Spline Approximation is more energy-effective than the “virtual gravity field” control method [8].

II. PARTICLE SWARM OPTIMIZATION

In the PSO algorithm, the trajectory of each individual in the search space is adjusted by dynamically altering the velocity of each particle, according to its own flying experience and the flying experience of other particles in the search space. The particles have a tendency to fly toward better search areas over the course of a search process. The standard PSO algorithm is given as follows [10]

$$V_{t+1} = wV_t + c_1 \text{rand}() (P_i - X_t) + c_2 \text{rand}() (P_g - X_t) \quad (1)$$

$$\mathbf{X}_{t+1} = \mathbf{X}_t + \mathbf{V}_{t+1} \quad (2)$$

Where $\text{rand}()$ generates uniformly distributed random numbers in the range $[0,1]$. w is called the inertia weight and is less than 1, \mathbf{V}_t and \mathbf{X}_t represent the speed and the position of the particle at time t respectively, \mathbf{P}_i refers to the best position found by the particle, and \mathbf{P}_g refers to the global best position found by the whole particle swarm. c_1 and c_2 are constants known as acceleration coefficients.

III. THE COMPASS GAIT BIPED MODEL

A. Dynamic Model of the Swing phase

The simplest model of a walking biped robot has two rigid legs, one joint is at the hip, and another joint is at the point where the support leg touches the ground, as shown in Fig. 1.

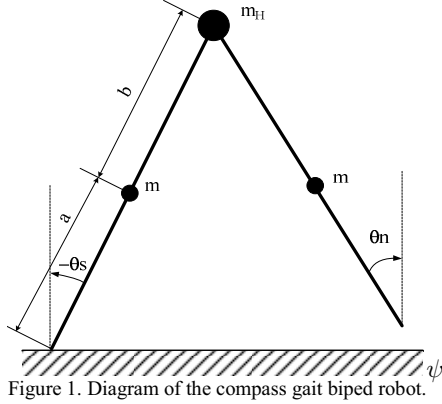


Figure 1. Diagram of the compass gait biped robot.

Mass of the biped robot is concentrated at three points: a hip mass m_H and two leg masses m . Values of these parameters are listed in Table I [7].

TABLE I. PARAMETERS FOR THE COMPASS GAIT BIPED

Parameter	Value	Description
m	5 kg	mass of each leg
m_H	10 kg	mass of the hip
a	0.5 m	distance between tip of leg and leg mass
b	0.5 m	distance between leg mass and hip
$l = a + b$	1 m	total length of leg
g	9.8 m/s ²	acceleration due to gravity

Each step of walking locomotion is divided into two phases; the walking mechanism is shown in Fig. 2. In the first phase, the swing leg swings from posture 1 to 2. When the swing leg touches the ground, the foot exchange takes place instantly from posture 2 to 3. The dynamic equation of the robot in the swing phase is given by

$$\mathbf{M}(\boldsymbol{\theta})\ddot{\boldsymbol{\theta}} + \mathbf{C}(\boldsymbol{\theta}, \dot{\boldsymbol{\theta}}) + \mathbf{g}(\boldsymbol{\theta}) = \boldsymbol{\tau} \quad (3)$$

where, $\boldsymbol{\theta} = [\theta_n, \theta_s]^T$, $\boldsymbol{\tau} = [\tau_n, \tau_s]^T$,

$$\mathbf{M}(\boldsymbol{\theta}) = \begin{pmatrix} mb^2 & -mlb \cos(\theta_n - \theta_s) \\ -mlb \cos(\theta_n - \theta_s) & (m_H + m) + ma^2 \end{pmatrix},$$

$$\mathbf{g}(\boldsymbol{\theta}) = \begin{pmatrix} mb \sin(\theta_n) \\ -(m_H l + ma + ml) \sin(\theta_s) \end{pmatrix} \text{ and}$$

$$\mathbf{C}(\boldsymbol{\theta}) = \begin{pmatrix} 0 & -mlb \sin(\theta_n - \theta_s) \dot{\theta}_s \\ mlb \sin(\theta_n - \theta_s) \dot{\theta}_n & 0 \end{pmatrix}.$$

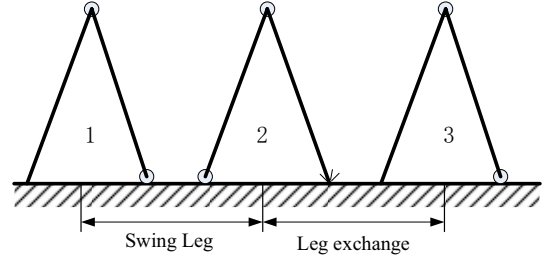


Figure 2. Diagram of the compass gait biped robot.

B. Ground impact

We can simplify the dynamics of the impact by making the following assumptions, which appear in the literature [7]:

1. The impact is perfectly plastic (no bounce occurs).
2. Support is instantaneously transferred from the stance leg to the swing leg.
3. The legs do not slip along the ground during the impact.

Under these assumptions, the impact results in an instantaneous change in angular velocities. We apply the law of conservation of angular momentum to relate the joint velocities before and after the impact. This result in

$$\mathbf{Q}^+(\alpha) \dot{\boldsymbol{\theta}}^+ = \mathbf{Q}^-(\alpha) \dot{\boldsymbol{\theta}}^- \quad (4)$$

Where $\alpha = (\theta_s^- - \theta_n^-) / 2$, superscripts “+” and “-” denote values before and after the impact respectively.

$$\mathbf{Q}^+(\alpha) = \begin{pmatrix} mb^2 - mbl \cos(2\alpha) & (ml^2 + ma^2 + m_H l^2) - mbl \cos(2\alpha) \\ mb^2 & -mbl \cos(2\alpha) \end{pmatrix}$$

$$\mathbf{Q}^-(\alpha) = \begin{pmatrix} -mab & [(2m + m_H)l - 2mb] \cos(2\alpha) - mab \\ 0 & -mab \end{pmatrix}.$$

According to (4), we can obtain the angular velocities relationship before and after the impact.

IV. CYCLIC WALKING GAIT PLANNING

A. Cyclic Walking condition

Here we derive the boundary conditions for the joint angular trajectories calculation in swing phase of the leg. In order to realize the cyclic walking gait, the state of robot at posture 3 must be the same as that at posture 1. Therefore we get

$$\boldsymbol{\theta}^0 = \boldsymbol{\theta}^+, \quad \dot{\boldsymbol{\theta}}^0 = \dot{\boldsymbol{\theta}}^+ \quad (5)$$

Where the superscript 0 denotes the initial state of the robot. According to (4) and (5), we can get the state of robot before the ground impact occurs

$$\boldsymbol{\theta}^- = \begin{bmatrix} 0 & 1 \\ 1 & 0 \end{bmatrix} \boldsymbol{\theta}^0, \quad \dot{\boldsymbol{\theta}}^- = [\mathbf{Q}^-(\alpha)]^{-1} \mathbf{Q}^+(\alpha) \dot{\boldsymbol{\theta}}^0 \quad (6)$$

B. The joint angular trajectories approximation

The joint angular trajectories in swing phase can be approximated by a cubic spline function as follows.

$$\boldsymbol{\theta} = \mathbf{f}(\boldsymbol{\theta}^0, \dot{\boldsymbol{\theta}}^0, \mathbf{p}, T) \quad (7)$$

Where \mathbf{p} is the parameter vector of a cubic spline function, and T is the period of cyclic walking. Substitute (7) into (3), we get the vector of control torques $\boldsymbol{\tau}$

$$\boldsymbol{\tau} = \boldsymbol{\Phi}(\boldsymbol{\theta}^0, \dot{\boldsymbol{\theta}}^0, \mathbf{p}, T) \quad (8)$$

C. Optimal Trajectory Planning Method Based on PSO

The walking locomotion in the first phase (the swing phase) is solved by the optimal trajectory planning method. In order to obtain a natural walking locomotion solution with the lowest possible input torque, the cost function is defined as the integral of the weighted sum of input torques's square,

$$J = \int_0^T (w_1 \tau_n^2 + w_2 \tau_s^2) dt \quad (9)$$

Where w_1 and w_2 are the weighted factors corresponding to the input torques τ_n and τ_s which can be calculated by (8). When the full-actuated system is desired, the weighted factors can be set as $w_1 = w_2$, otherwise when the under-actuated system is desired, the weighted factor can be set larger for the under-actuated joint. It is very difficult to set a joint as a strict under-actuated joint by trajectory planning method. Even if an input torque was set as zero in the optimal trajectory planning method, the simulation results generated by the system showed that this torque is not zero, and sometimes it is larger than the input torques applied on the other joints [9]

The optimal trajectory planning problem can be described as follows

$$\min J(\mathbf{x}) = \int_0^T (w_1 \tau_n^2 + w_2 \tau_s^2) dt \quad (10)$$

Where $\mathbf{x} = [\boldsymbol{\theta}^0, \dot{\boldsymbol{\theta}}^0, \mathbf{p}]^T$, and the cyclic walking period T are selected according to passive dynamic walking (PDW). The optimal trajectory is obtained by solving \mathbf{x} that minimizes the value of J in (10). When \mathbf{x} is obtained, the joint angular trajectories and the vector of control torques can be calculated by (7) and (8) respectively.

The Newton-Raphson iteration method is usually used to solve the optimal trajectory planning problem [9]. But the complex difference calculations are needed in Newton-Raphson iteration method and it is sensitive to the initial value. For different initial values, different local optima can be obtained. So the PSO algorithm introduced in section II is utilized to solve the optimal trajectory planning problem. Difference calculations are not needed in the PSO algorithm.

Using (1) and (2), the pseudo code of the PSO algorithm for the optimal trajectory planning problem is as follows

```

Begin
  initialize the population and the parameter
  while(the error of the trajectory end-point < ε)
    for(i=1 to N)
      calculate the fitness  $F(\mathbf{X}_i)$ , update  $\mathbf{P}_i$  and  $\mathbf{P}_g$ 
       $\mathbf{V}_{i+1} = w\mathbf{V}_i + c_1 \text{rand}() (\mathbf{P}_i - \mathbf{X}_i) + c_2 \text{rand}() (\mathbf{P}_g - \mathbf{X}_i)$ 
       $\mathbf{X}_{i+1} = \mathbf{X}_i + \mathbf{V}_{i+1}$ 
    increase i
  end while
end.
```

Where N is the number of particles in the PSO algorithm.

V. SIMULATION RESULTS

The PSO algorithm for optimal trajectory planning is examined using the compass gait biped robot model which has been introduced in section III. For a real compass gait biped robot system, the actuate torques are always acted on hip joint and ankle joint of the stance leg. So the torques for stance and swing legs are dependent each other. The ankle torque and hip torque can be calculated as follows

$$\tau_{hip} = \tau_n, \tau_{ankle} = \tau_s + \tau_n \quad (11)$$

The input torques in optimal trajectory planning problem (10) are replaced by ankle torque and hip torque when the simulation is performed. In all tests the time period T is set as $T = 0.7347s$, which is the period in PDW at a 3° slope. The parameters for PSO algorithm are selected as follows: inertia weight $w = 0.729$, and acceleration coefficients $c_1 = c_2 = 1.494$. The number of particles in the PSO algorithm is set as 15.

Case 1: The interval $[0, T]$ is divided into 6 equal subintervals, the maximum number of iterations is set as 1000. The weighted factors corresponding to the input torques are set as $w_1 = w_2 = 1$. The energy of the optimal trajectory equals to 43.9692 units. The optimal control torques and the resulting optimal trajectory are presented in Fig. 3(a) and Fig. 3(b) respectively. In Fig.3 (a), the solid line denotes the ankle torque and the dash line denotes the hip torque. In Fig. 3(b), the solid line denotes the phase plot of the stance leg and the

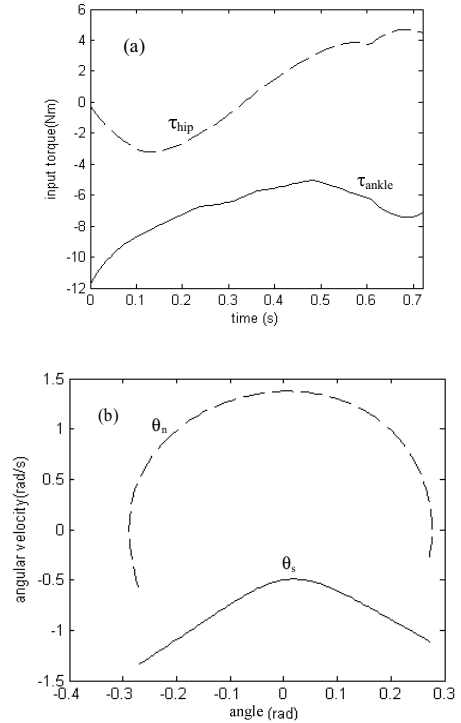


Figure 3. Results of optimal trajectory planning generated by the PSO algorithm $w_1 = w_2 = 1$ (a) Optimal control torques (b) optimal trajectory.

dish line denotes the phase plot of the non-stance leg.

Case 2: The interval $[0, T]$ is divided into 2 equal subintervals, and the other parameters are set the same as in Case 1.

The energy of the optimal trajectory equals to 43.4578 units. The optimal control torques and the resulting optimal trajectory are presented in Fig. 4(a) and Fig. 4(b) respectively. In Fig. 4(a), the solid line denotes the ankle torque and the dish line denotes the hip torque. In Fig. 4(b), the solid line denotes the phase plot of the stance leg and the dish line denotes the phase plot of the non-stance leg.

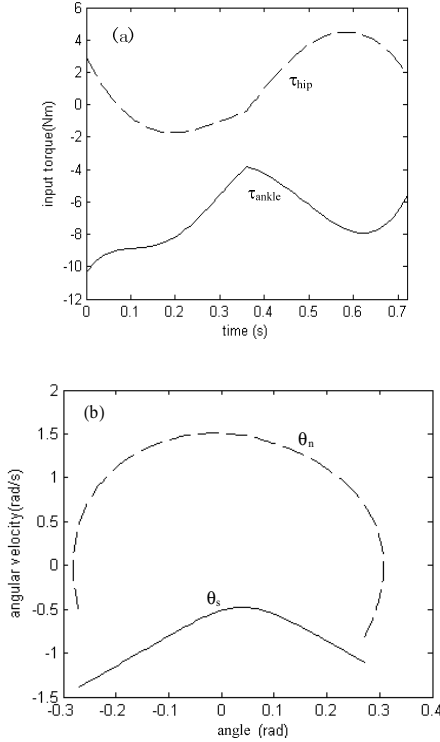


Figure 4. Results of optimal trajectory planning generated by the PSO algorithm $w_1 = w_2 = 1$ (a) Optimal control torques (b) optimal trajectory.

Comparing case 1 with case 2, it can be found that the values of the performance index are similar in the two cases and optimal control torques and optimal trajectories are similar also. So in order to reduce the calculating amount, the interval $[0, T]$ is divided into 2 equal subintervals in the later simulations.

Case 3: The weighted factors corresponding to the input torques are set as $w_1 = 1$ and $w_2 = 10$. The other parameters are set the same as in Case 2.

The energy of the optimal trajectory equals to 304.9114 units. The optimal control torques and the resulting optimal trajectory are presented in Fig. 5(a) and Fig. 5(b) respectively. Comparing Fig. 5 with Fig. 4, it can be found that the ankle torque can be reduced by increasing the weighted factor w_2 , but the phase plot of the non-stance leg is irregular. If the weighted factor w_2 is increased furthermore, no stable result can be obtained.

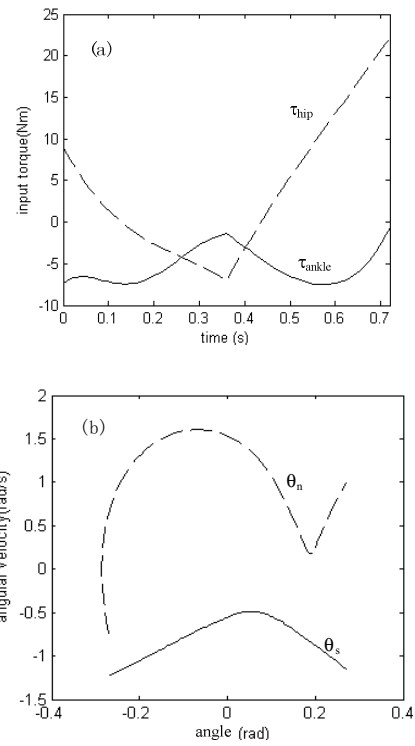


Figure 5 Results of optimal trajectory planning generated by the PSO algorithm $w_1 = 1$ and $w_2 = 10$ (a) Optimal control torques (b) optimal trajectory.

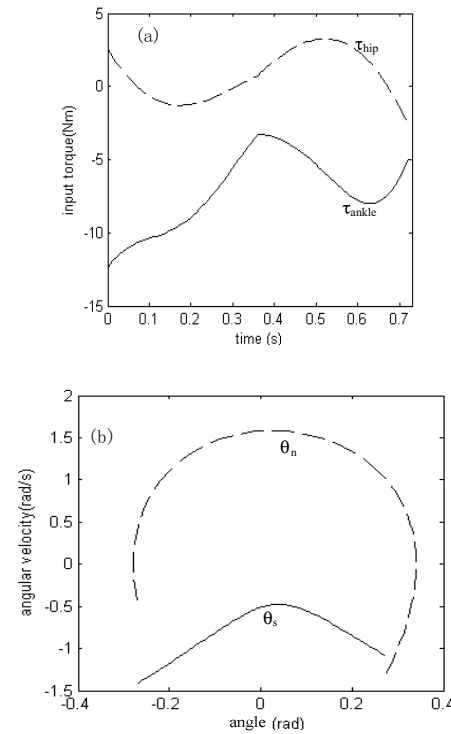


Figure 6. Results of optimal trajectory planning generated by the PSO algorithm $w_1 = 10$ and $w_2 = 1$ (a) Optimal control torques (b) optimal trajectory.

Case 4: The weighted factors corresponding to the input torques are set as $w_1=10$ and $w_2=1$. The other parameters are set the same as in Case 2.

The energy of the optimal trajectory equals to 68.7693 units. The optimal control torques and the resulting optimal trajectory are presented in Fig. 6(a) and Fig. 6(b) respectively.

Case 5: The weighted factors corresponding to the input torques are set as $w_1=1000$ and $w_2=1$. The other parameters are set the same as in Case 2.

The energy of the optimal trajectory equals to 936.1651 units. The optimal control torques and the resulting optimal trajectory are presented in Fig. 7(a) and Fig. 7(b) respectively. Fig. 7(a) shows that the hip joint is approximately passive when the weighted factor for hip joint torque is large enough.

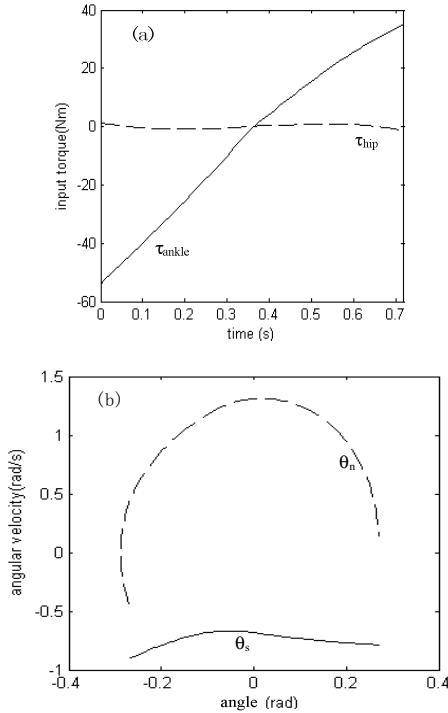


Figure 7. Results of optimal trajectory planning generated by the PSO algorithm $w_1=1000$ and $w_2=1$ (a) Optimal control torques (b) optimal trajectory

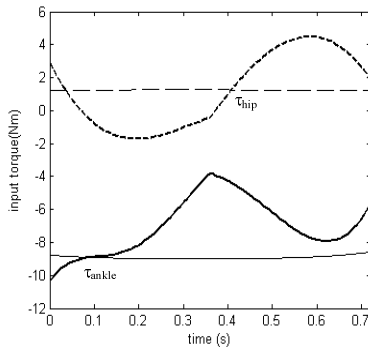


Figure 8. Control torques comparing, the optimal control torques are shown in thick line, and control torques of the virtual gravity are shown in thin line.

Fig. 8 show the control torques generated by optimal trajectory planning method and virtual gravity method [8]. The thick line represents the control torques which are the same as that in Fig.4 (a), and the thin line represents the control torques generated by the virtual gravity method. The energy of virtual gravity method equals to 59.391 units, which is higher than 43.4578 units in the optimal trajectory planning method.

VI. CONCLUSION

In this paper, the optimal trajectory planning method with the least square input torque for a compass gait biped robot is proposed. The trajectory solution that satisfies both the optimized condition and the cyclic motion is obtained by PSO algorithm and spline approximation. We also attempted to get the optimal solution under an under-actuated condition by using a large weighted factor. Several simulations are performed in difference conditions. From the simulation results, we can conclude as follows:

1. The optimal trajectory planning method adopted in this paper is effective to solve the optimal walking gait that minimizes the integral of input torque's square.
2. If we make one joint be under-actuated, we can let the corresponding weighted factor be larger enough. For a compass gait biped robot, the hip joint can be designed to be approximately passive. But it is a difficult task to make the ankle joint passive. Strict passive joint is very difficult for the optimal trajectory planning method, and sometimes the real joint torque may be very large [9]. But the approximately passive feature is also worthful for designing a robot, and a small motor can be used to reduce the joint weight. Fig. 7(a) shows that the hip joint is approximately passive, but the ankle torque is increased greatly (see the result in Fig. 4(a)).
3. The optimal trajectory planning method proposed in this paper is more energy-effective than the virtual gravity method.

ACKNOWLEDGMENT

This work was supported in part by the National Natural Science Foundation of China (10772020), Scientific Research Common Program of Beijing Municipal Commission of Education (KM200910772025) and Funding Project for Academic Human Resources Development in Institutions of Higher Learning Under the Jurisdiction of Beijing Municipality (PHR201007130).

REFERENCES

- [1] M.Vukobratovic, B. Borovac, "Zero-Moment point, thirty-five years of its Lif," International Journal of Humanoid Robot, 2004, 1(1): 157-173
- [2] H Hirukawa, S. Kajita, F. Kanehiro, K. Kaneko, "The human-size humanoid robot that can walk, lie down and get up," International Journal of Robotics Research, 2005, 24(9): 755-769..
- [3] K. Hirai, et al., "The development of Honda Humanoid Robot," Proc. IEEE Int. Conf. Robotics and Automation, Leuven, Belgium, 1998, pp. 983-985..
- [4] S.Collins, A. Ruina, R. Tedrake, and M. Wisse, "Efficient bipedal robots based on passive dynamic walkers," Science, 2005, 307: 1082-1085.
- [5] Vanderborght et al., "Comparison of Mechanical Design and Energy Consumption of Adaptable, Passive-compliant Actuators," The International Journal of Robotics Research, 2009, 28(1): 90-103.
- [6] T. McGeer, "Passive dynamic walking," International Journal Robotics Research, 1990, 9(2): 62-82.

- [7] J. K. Holm, "Control of passive-dynamic robots using artificial potential energy fields," Urbana, Illinois: University of Illinois at Urbana-Champaign, 2005.
- [8] M. Yamakita, F. Asano and K. Furuta, "Passive velocity field control of biped walking robot," Proc. The Int. Conf. Robotics and Automation, 2000, pp. 3057-3062.
- [9] K. Ono and R. Liu, "Optimal Biped Walking Locomotion Solved by Trajectory Planning Method," ASME Journal of Dynamic Systems, Measurement, and Control, 2002, 124(3): 554-565.
- [10] A. Ratnaweera, S. K. Halgamuge and H. C. Watson, "Self-organizing hierarchical particle swarm optimizer with time-varying acceleration coefficients," IEEE Trans on Evolutionary Computation, 2004, 8(3): 240-255.